SINUSOIDAL VOLTAGE CLAMP OF THE HODGKIN–HUXLEY MODEL

RICHARD FITZHUGH
Laboratory of Biophysics, National Institute of Neurological and Communicative Disorders and Stroke, National Institutes of Health, Bethesda, Maryland 20205

ABSTRACT A voltage clamp consisting of a sinusoidal voltage of amplitude V_1 and frequency f, superimposed on a steady voltage level V_0, is applied to the Hodgkin-Huxley model of the squid giant axon membrane. The steady-state response is a current composed of sinusoidal components of frequencies $0, f, 2f, 3f, \ldots$ The frequencies greater than f arise from the nonlinearity of the membrane. The total current is described by a power series in V_1; each coefficient of this series is composed of current components for one or more frequencies. For different frequencies one can derive higher-order generalized admittances characterizing the nonlinear as well as the linear properties of the membrane. Formulas for the generalized admittances are derived from the Hodgkin-Huxley equations for frequencies up to $3f$, using a perturbation technique. Some of the resulting theoretical curves are compared with experimental results, with good qualitative agreement.

INTRODUCTION

DeFelice et al. (1980, 1981) and Moore et al. (1980) have measured the response of the squid giant axon membrane to a sinusoidal voltage clamp. In these experiments the voltage-clamp waveform consists of a constant potential step, with a sinusoidal potential of frequency f superimposed on it. After the initial transients have decayed, a steady-state current is measured, consisting of a constant current plus sinusoidal components at frequencies f, $2f$, $3f, \ldots$. The amplitudes and phases of these components are computed from the records by Fourier analysis.

DERIVATION OF EQUATIONS

In this paper theoretical equations are derived for comparison with their results. A preliminary account of this work has been published (FitzHugh, 1981).

Each of the variables m, h, n in the Hodgkin-Huxley (HH) model obeys a differential equation of the form

$$\dot{x} = \mathrm{d}x/\mathrm{d}t = \phi\,[\alpha_x(V) - \gamma_x(V)\,x], \tag{1}$$

where V is the membrane potential and x is m, h, or n. ϕ is a positive constant which depends on the temperature, and $\gamma_x(V) = \alpha_x(V) + \beta_x(V)$. For a voltage clamp in which $V = V_0$ = constant, $\dot{x} = 0$ in the steady state, and x has a constant value:

$$x = x_0 = \alpha_x(V_0)/\gamma_x(V_0). \tag{2}$$

Add a sinusoidal signal to V_0, so that

$$V = V_0 + V_1 \cos(\omega t), \qquad \omega = 2\pi f,$$

where V_1 is the amplitude and f the frequency of the sinusoid. In response to this potential, after the decay of any transients resulting from the initiation of the sinusoidal clamp, $x(t)$, the solution of Eq. 1 approaches a periodic steady-state waveform. Because $\alpha_x(V)$ and $\gamma_x(V)$ vary with V, $x(t)$ in general contains components of frequencies (harmonics) that are multiples of f (the fundamental), as well as a DC offset- or zero-frequency component. For small V_1, the fundamental component predominates, but as V_1 increases, the amplitudes of the other components increase, relative to that of the fundamental. These harmonics in m, h, n are reflected in the current waveform recorded from the voltage clamp.

To derive expressions for the various frequency components of $x(t)$, the solution of Eq. 1 is expanded in a power series in V_1

$$x(t) = x_0 + V_1 x_1 + V_1^2 x_2 + V_1^3 x_3 + \cdots, \tag{3}$$

where x_1, x_2, x_3 are functions of t only.

Because of the complexity of some of the equations derived below, several special notations have been devised. They are intended to be compact but reasonably comprehensible. The first such notation is to let $c_k = \cos(k\omega t)$, $s_k = \sin(k\omega t)$, for $k = 0, 1, 2, 3, \ldots$. The following relations are useful:

$$\begin{aligned} &c_0 = 1, \quad s_0 = 0, \quad c_{-k} = c_k, \quad s_{-k} = -s_k, \\ &c_j c_k = (c_{j-k} + c_{j+k})/2, \\ &c_j s_k = (s_{j+k} - s_{j-k})/2 \\ &s_j s_k = (c_{j-k} - c_{j+k})/2 \\ &dc_k/dt = -k\,\omega\,s_k, \qquad ds_k/dt = k\,\omega\,c_k. \end{aligned} \tag{4}$$

Power series for V, $\dot{x}$, $\alpha_x(V)$, $\gamma_x(V)$ are

$$\begin{aligned} V &= V_0 + V_1 c_1 \\ \dot{x} &= V_1 \dot{x}_1 + V_1^2 \dot{x}_2 + V_1^3 \dot{x}_3 + \cdots \\ \alpha_x(V) &= \alpha + V_1 \alpha' c_1 + V_1^2 \alpha'' c_1^2/2 \\ &\quad + V_1^3 \alpha''' c_1^3/6 + \cdots \\ \gamma_x(V) &= \gamma + V_1 \gamma' c_1 + V_1^2 \gamma'' c_1^2/2 \\ &\quad + V_1^3 \gamma''' c_1^3/6 + \ldots . \end{aligned} \tag{5}$$

Here the primes indicate differentiation with respect to V; α, α', α'', α''' denote $\alpha_x(V)$ and its derivatives evaluated at $V = V_0$ (similarly for γ).

The product $\gamma_x(V)\, x$ in Eq. 1 becomes, using Eqs. 3, 5

$$\begin{aligned} \gamma_x(V)\, x &= \gamma x_0 + V_1(\gamma x_1 + \gamma' x_0 c_1) \\ &\quad + V_1^2(\gamma x_2 + \gamma' x_1 c_1 + \gamma'' x_0 c_1^2/2) \\ &\quad + V_1^3(\gamma x_3 + \gamma' x_2 c_1 + \gamma'' x_1 c_1^2/2 \\ &\quad + \gamma''' x_0 c_1^3/6) + \cdots . \end{aligned} \tag{6}$$

Substituting from Eq. 3, 5, 6 into Eq. 1 gives a separate equation for each power V_1^k of V_1. For V_1^0

$$0 = \phi(\alpha - \gamma x_0),$$

which agrees with Eq. 2. For V_1^1

$$\dot{x}_1 = \phi(\alpha' c_1 - \gamma x_1 - \gamma' x_0 c_1). \tag{7}$$

The general steady-state solution of this equation has the form

$$x_1 = x_1^{c1} c_1 + x_1^{s1} s_1, \tag{8}$$

where x_1^{c1}, x_1^{s1} are constants. The subscript of each such constant is the same as the subscript of x on the left side of the equation. The superscript (c or s followed by a digit) indicates whether it is a coefficient of a cosine or of a sine; the digit is the same as the subscript of c or s, and indicates the order of the harmonic. Substitute Eq. 8 into Eq. 7, and separate into two independent equations, one containing only terms in c_1, the other only in s_1. For all k, let

$$D_k = \phi^2 \gamma^2 + k^2 \omega^2.$$

Solving the two equations just obtained for x_1^{c1}, x_1^{s1} gives

$$\begin{aligned} x_1^{c1} &= \phi \gamma A_{11}/D_1 \\ x_1^{s1} &= \omega A_{11}/D_1, \end{aligned}$$

where $A_{11} = \phi(\alpha' - \gamma' x_0)$.

For V_1^2

$$\dot{x}_2 = \phi(\alpha'' c_1^2/2 - \gamma x_2 - \gamma' x_1 c_1 - \gamma'' x_0 c_1^2/2), \tag{9}$$

let

$$x_2 = x_2^{c0} c_0 + x_2^{c2} c_2 + x_2^{s2} s_2. \tag{10}$$

Substitute Eqs. 8, 10 into Eq. 9. Eliminate all products of c_k, s_k, using Eq. 4. Three equations result, one each for c_0, c_2, and s_2. Solve these to give

$$\begin{aligned} x_2^{c0} &= A_{22}/(\phi \gamma) \\ x_2^{c2} &= (\phi \gamma A_{22} - 2\omega B_{22})/D_2 \\ x_2^{s2} &= (2\omega A_{22} + \phi \gamma B_{22})/D_2, \end{aligned}$$

where

$$\begin{aligned} A_{22} &= \phi[(\alpha'' - \gamma'' x_0)/4 + \gamma' x_1^{c1}/2] \\ B_{22} &= -\phi \gamma' x_1^{s1}/2. \end{aligned}$$

For V_1^3

$$\dot{x}_3 = \phi(\alpha''' c_1^3/6 - \gamma x_3 - \gamma' x_2 c_1 - \gamma'' x_1 c_1^2/2 - \gamma''' x_0 c_1^3/6).$$

Let

$$x_3 = x_3^{c1} c_1 + x_3^{s1} s_1 + x_3^{c3} c_3 + x_3^{s3} s_3. \tag{11}$$

Proceeding as before,

$$\begin{aligned} x_3^{c1} &= (\phi \gamma A_{31} - \omega B_{31})/D_1 \\ x_3^{s1} &= (\omega A_{31} + \phi \gamma B_{31})/D_1 \\ x_3^{c3} &= (\phi \gamma A_{33} - 3\omega B_{33})/D_3 \\ x_3^{s3} &= (3\omega A_{33} + \phi \gamma B_{33})/D_3 \end{aligned}$$

where

$$\begin{aligned} A_{31} &= \phi[(\alpha''' - \gamma''' x_0)/8 - \gamma'(2 x_2^{c0} + x_2^{c2})/2 - 3\gamma'' x_1^{c1}/8] \\ B_{31} &= \phi[-\gamma' x_2^{s2}/2 - \gamma'' x_1^{s1}/8] \\ A_{33} &= \phi[(\alpha''' - \gamma''' x_0)/24 - \gamma' x_2^{c2}/2 - \gamma'' x_1^{c1}/8] \\ B_{33} &= B_{31}. \end{aligned}$$

One could continue this process for higher powers of V_1, resulting in more and more complicated expressions. The pattern that emerges is that x_k, the coefficient of V_1^k in the power series for x, can be expressed as a sum of terms in the cosines c_j and sines s_j for certain frequencies jf. If k is even, j is even and ranges from 0 to k; if k is odd, j is odd, from 1 to k. The coefficients x_k^{cj} of c_j and x_k^{sj} of s_j in the expression for x_k can be calculated from α, γ, and their derivatives, evaluated at V_0, and recursively from the x_i^{cj}'s and x_i^{sj}'s for $i < k$.

The periodic variations of m, h, n (found by substituting m, h, n for x in the above expressions) in turn produce periodic variations in the total membrane current. The next step is to find the amplitudes and phases of these current components at each frequency, as functions of V_1. The total membrane current and ionic current of the HH model are

$$I = C\dot{V} + J(V, m, h, n) \tag{12}$$

$$J(V, m, h, n) = \bar{g}_{Na} m^3 h(V - V_{Na}) + \bar{g}_K n^4 (V - V_K) + g_L(V - V_L). \tag{13}$$

C is the membrane capacitance.

The power series for V, $\dot{V}$, m, h, n are

$$\begin{aligned} V &= V_0 + V_1 c_1 \\ \dot{V} &= -V_1 \omega s_1 \\ m &= m_0 + V_1 m_1 + V_1^2 m_2 + V_1^3 m_3 + \cdots \\ h &= h_0 + V_1 h_1 + V_1^2 h_2 + V_1^3 h_3 + \cdots \\ n &= n_0 + V_1 n_1 + V_1^2 n_2 + V_1^3 n_3 + \cdots \end{aligned} \tag{14}$$

Partial derivatives of J, taken with respect to one or more variables (V, m, h, n), will be indicated by subscripts to J, e.g., J_m, J_{mh}, J_{nnn}. All derivatives are evaluated at V_0, m_0, h_0, n_0. Let $\delta V = V - V_0$, $\delta m = m - m_0$, $\delta h = h - h_0$, $\delta n = n - n_0$, $\delta x = x - x_0$.

To avoid unnecessary repetition of similar terms the following notation is used. Wherever x appears in an expression, the latter represents a sum of terms in which m, h, n are substituted for x. For example,

$$\begin{aligned} \delta x\, J_x &= \delta m\, J_m + \delta h\, J_h + \delta n\, J_n \\ J_x x_1^{c1} &= J_m m_1^{c1} + J_h h_1^{c1} + J_n n_1^{c1} \\ J_{xx}(x_1^{c1})^2 &= J_{mm}(m_1^{c1})^2 + J_{nn}(n_1^{c1})^2. \end{aligned}$$

The third equation contains no term with $x = h$, because, from Eq. 13, $J_{hh} = 0$.

Expand J in a multivariate Taylor series in δV, δx ($x = m, h, n$)

$$\begin{aligned} J = J_0 &+ [\delta V J_V + \delta x J_x] \\ &+ (1/2)[(\delta x)^2 J_{xx} + 2\,\delta V\,\delta x\, J_{Vx} + 2\,\delta m\,\delta h\, J_{mh}] \\ &+ (1/6)[(\delta x)^3 J_{xxx} + 3\,\delta V(\delta x)^2 J_{Vxx} \\ &\qquad + 3(\delta m)^2 \delta h\, J_{mmh} + 6\,\delta V\,\delta m\,\delta h\, J_{Vmn}] \\ &+ \cdots . \end{aligned} \tag{15}$$

Power series in V_1 (up to V_1^3) for the linear terms $\delta V, \ldots, \delta n$ in Eq. 15 are found from Eq. 14. Series for quadratic terms $(\delta m)^2, \ldots, \delta m\,\delta h$ and for cubic terms $(\delta m)^3, \ldots, \delta V\,\delta m\,\delta h$ are then found by multiplying two or three of these power series together. For example,

$$\begin{aligned} (\delta m)^2 &= V_1^2 m_1^2 + 2V_1^3 m_1 m_2 + \cdots \\ \delta V\,\delta m &= V_1^2 m_1 c_1 + V_1^3 m_2 c_1 + \cdots \\ (\delta m)^3 &= V_1^3 m_1^3 + \cdots \\ \delta V\,\delta m\,\delta h &= V_1^3 m_1 h_1 c_1 + \cdots \end{aligned} \tag{16}$$

Terms like those in Eq. 16 are then expressed in terms of powers of c_k, s_k by substituting for the coefficients m_j^{ck}, m_j^{sk}, etc., from Eqs. 8, 10, 11. For example,

$$\begin{aligned} \delta V\,\delta m &= V_1^2(m_1^{c1} c_1 + m_1^{s1} s_1)c_1 \\ &\quad + V_1^3(m_2^{c0} c_0 + m_2^{c2} c_2 + m_2^{s2} s_2)c_1 + \cdots \\ (\delta m)^3 &= V_1^3(m_1^{c1} c_1 + m_1^{s1} s_1)^3 + \cdots . \end{aligned}$$

The resulting products of c_k's and s_k's are then converted to linear terms in the c_k's and s_k's, using Eq. 4. Substituting these expressions into Eq. 15 and then into Eq. 12 gives a power series in V_1 for I:

$$I = I_0 + V_1 I_1 + V_1^2 I_2 + V_1^3 I_3 + \cdots \tag{17}$$

where

$$I_0 = J_0 \tag{18}$$

$$\begin{aligned} I_1 &= I_1^{c1} c_1 + I_1^{s1} s_1 \\ I_1^{c1} &= J_V + J_x x_1^{c1}, \qquad I_1^{s1} = -\omega C + J_x x_1^{s1}. \end{aligned} \tag{19}$$

The previous superscript notation is extended to allow multiple superscripts, indicating a coefficient of products of c_k, s_k. For example, I_2^{c1c1s1} is the coefficient of $(c_1)^2 s_1$ in the expression for I_2. Also, let $MH_{jk}^{XY} = m_j^X h_k^Y + m_k^Y h_j^X$, *where* $j, k = 1$ or 2 and $X, Y = ci$ or si for some integer i. For example,

$$MH_{12}^{c1s2} = m_1^{c1} h_2^{s2} + m_2^{s2} h_1^{c1}.$$

Using these notations,

$$\begin{aligned} I_2 &= I_2^{c0} + I_2^{c2} c_2 + I_2^{s2} s_2 \\ I_2^{c0} &= J_x x_2^{c0} + (1/2)(I_2^{c1c1} + I_2^{s1s1}) \\ I_2^{c2} &= J_x x_2^{c2} + (1/2)(I_2^{c1c1} - I_2^{s1s1}) \\ I_2^{s2} &= J_x x_2^{s2} + (1/2) I_2^{c1s1} \\ I_2^{c1c1} &= J_{Vx} x_1^{c1} + (1/2) J_{xx}(x_1^{c1})^2 + J_{mh} m_1^{c1} h_1^{c1} \\ I_2^{c1s1} &= J_{Vx} x_1^{s1} + J_{xx} x_1^{c1} x_1^{s1} + J_{mh} MH_{11}^{c1s1} \\ I_2^{s1s1} &= (1/2) J_{xx}(x_1^{s1})^2 + J_{mh} m_1^{s1} h_1^{s1}. \end{aligned} \tag{20}$$

$$\begin{aligned} I_3 &= I_3^{c1} c_1 + I_3^{s1} s_1 + I_3^{c3} c_3 + I_3^{s3} s_3 \\ I_3^{c1} &= J_x x_3^{c1} + J_{Vx} x_2^{c0} + J_{xx} x_1^{c1} x_2^{c0} \\ &\quad + J_{mh} MH_{12}^{c1c0} + (1/2)(I_3^{c1c2} + I_3^{s1s2}) \\ &\quad + (1/4)(3 I_3^{c1c1c1} + I_3^{c1s1s1}) \\ I_3^{s1} &= J_x x_3^{s1} + J_{xx} x_1^{s1} x_2^{c0} + J_{mh} MH_{12}^{s1c0} \\ &\quad + (1/2)(I_3^{c1s2} - I_3^{s1c2}) + (1/4)(I_3^{c1c1s1} + 3 I_3^{s1s1s1}) \\ I_3^{c3} &= J x_3^{c3} + (1/2)(I_3^{c1c2} - I_3^{s1s2}) \\ &\quad + (1/4)(I_3^{c1c1c1} - I_3^{c1s1s1}) \\ I_3^{s3} &= J_x x_3^{s3} + (1/2)(I_3^{c1s2} + I_3^{s1c2}) \\ &\quad + (1/4)(I_3^{c1c1s1} - I_3^{s1s1s1}) \\ I_3^{c1c2} &= J_{Vx} x_2^{c2} + J_{xx} x_1^{c1} x_2^{c2} + J_{mh} MH_{12}^{c1c2} \\ I_3^{c1s2} &= J_{Vx} x_2^{s2} + J_{xx} x_1^{c1} x_2^{s2} + J_{mh} MH_{12}^{c1s2} \\ I_3^{s1c2} &= J_{xx} x_1^{s1} x_2^{c2} + J_{mh} MH_{12}^{s1c2} \\ I_3^{s1s2} &= J_{xx} x_1^{s1} x_2^{s2} + J_{mh} MH_{12}^{s1s2} \\ I_3^{c1c1c1} &= (1/2) J_{Vxx}(x_1^{c1})^2 + J_{Vmh} m_1^{c1} h_1^{c1} \\ &\quad + (1/6) J_{xxx}(x_1^{c1})^3 + (1/2) J_{mmh}(m_1^{c1})^2 h_1^{c1} \end{aligned}$$

$$I_3^{c1c1s1} = J_{Vxx} x_1^{c1} x_1^{s1} + J_{Vmh} M H_{11}^{c1s1}$$
$$+ (1/2) J_{xxx} (x_1^{c1})^2 x_1^{s1}$$
$$+ (1/2) J_{mmh} m_1^{c1} (m_1^{c1} h_1^{s1} + 2 m_1^{s1} h_1^{c1})$$
$$I_3^{c1s1s1} = (1/2) J_{Vxx} (x_1^{s1})^2 + J_{Vmh} m_1^{s1} h_1^{s1}$$
$$+ (1/2) J_{xxx} x_1^{c1} (x_1^{s1})^2$$
$$+ (1/2) J_{mmh} m_1^{s1} (2 m_1^{c1} h_1^{s1} + m_1^{s1} h_1^{c1})$$
$$I_3^{s1s1s}1 = (1/6) J_{xxx} (x_1^{s1})^3 + (1/2) J_{mmh} (m_1^{s1})^2 h_1^{s1}. \quad (21)$$

By using these special notations, it has been possible to compress the above equations into a reasonable space.

COMPARISON WITH EXPERIMENTS

The quantities I_1^{c1} and $-I_1^{s1}$ (note the negative sign) are the real and imaginary part of the conventional linear admittance (FitzHugh, 1981). When they are plotted as coordinates of a complex plane for a curve in which the frequency f is varied from zero to infinity, for a particular value of V_0, the curve is called an admittance locus.

By analogy, the other quantities I_k^j and $-I_k^j$, for $k > 1$, taken in pairs, can be considered as the components of generalized admittances of higher order, with the units $\mu A\ cm^{-2}\ mV^{-k}$. The term "admittance" usually refers to a linear response. Its use in this generalized sense, to characterize the current as a nonlinear function of voltage input, is unconventional, but should cause no confusion if the above definitions are kept in mind. Generalized admittance loci have been published elsewhere (FitzHugh, 1981) and are not considered further in this paper.

De Felice et al. (1981) describe experiments in which the currents were measured for different amplitudes (V_1) of the voltage sinusoid in a voltage clamp. Instead of trying to gather data at a wide range of frequencies, they concentrated primarily on one particular one, which they call the "zero phase" frequency. They define this as the frequency at which the current sinusoid at the fundamental frequency is exactly in phase with the voltage sinusoid. The linear admittance is then real; at that frequency, the linear admittance locus crosses the real axis of the complex plane to the right of the origin. Such loci for the HH model (FitzHugh, 1981, Fig. 1) can however cross the real axis either to the right or to the left of the origin. If to the left, the phase angle is not 0°, but 180° (FitzHugh, 1981). This is one difference between the model and the experiments of DeFelice et al. (1981); in the latter, 180° phase shifts did not occur. However, a 180° phase shift was reported by Fishman et al. (1979). In their experiments, the input voltage was not a sinusoid, but a sample of broad-band pseudorandom noise containing many frequencies, and the linear response at separate frequencies was obtained by computation using Fourier analysis. Moreover, the potassium current was suppressed in their experiments by perfusion with CsF solution; the negative conductance of the remaining sodium current presumably produced this

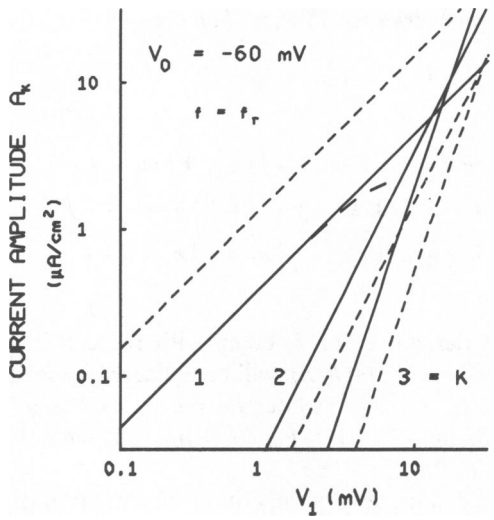

FIGURE 1 The amplitude A_k of the component of current at frequency kf_r (k = 1, 2, 3), plotted against the amplitude V_1 of the voltage sinusoid, with logarithmic coordinates on both axes. Solid straight lines with slope k are the linear approximation resulting from the first two terms in Eq. 23. The short dashed curve shows the departure from the k = 1 straight line due to the next higher (quadratic) term in the theoretical power series. Broken lines are experimental data (see text). f_r = 54 Hz (theoretical), 62.2 Hz (experimental).

180° phase shift. This 0° or 180° phase frequency is denoted here as f_r (r for real admittance).

With V_0 and f_r fixed, DeFelice et al. (1981) recorded the current waveform at different values of the input amplitude V_1, and separated it into components at frequencies $f = f_r, 2f_r$, and $3f_r$, using Fourier analysis. The amplitudes of the resulting current components were then plotted against V_1. With logarithmic scales on both axes, the result is approximately a straight line for each frequency, with a slope that is equal to the order (Eqs. 1, 2, or 3).

It was not obvious to the experimenters why these values of the slopes should occur, but a theoretical explanation can be found from Eqs. 17–21. The amplitude of the sinusoidal component of the total current I at the fundamental frequency f is:

$$A_1 = \{[V_1 I_1^{c1} + V_1^3 I_3^{c1} + 0(V_1^5)]^2$$
$$+ [V_1 I_1^{s1} + V_1^3 I_3^{s1} + 0(V_1^5)]^2\}^{1/2}$$
$$= \{V_1^2[(I_1^{c1})^2 + (I_1^{s1})^2] + 2V_1^4[I_1^{c1} I_3^{c1} + I_1^{s1} I_3^{s1}]$$
$$+ 0(V_1^6)\}^{1/2}.$$

Here the conventional notation $O(V_1^n)$ is used to denote unspecified terms of degree n and higher in V_1. Define $|I_k|$, the amplitude of the kth order admittance at frequency kf, as follows:

$$|I_k| = [(I_k^k)^2 + (I_k^k)^2]^{1/2}, \qquad k = 1, 2, 3. \quad (22)$$

Then

$$A_1 = |I_1| V_1 [1 + 0(V_1^2)].$$

Proceeding similarly with the sinusoidal currents at frequencies $2f$ and $3f$, and taking logarithms of both sides of the resulting equations, gives the general result:

$$\log(A_k) = \log(|I_k|) + k \log(V_1) + 0(V_1^2),$$
$$k = 1, 2, 3 \qquad (23)$$

where A_k is the amplitude of the sinusoidal component of I at frequency kf.

If A_k is plotted against V_1 on a log-log plot, the first two terms on the right predominate for small V_1, and that part of the curve is very nearly a straight line with slope k. As V_1 increases, the third- and higher-order terms become appreciable, and the curve departs noticeably from the straight line (see short broken curve in Fig. 1).

Figs. 1 and 2 show such straight lines. Similar lines were found experimentally by Moore et al. (1980, Fig. 6). However, the slope of their curve for $k = 2$ is ~1.5 rather than 2, and for $k = 3$ and 4, ~3.5. In their experiments, the sodium current was suppressed by external TTX solution, leaving the potassium current.

The solid lines in Fig. 1 were computed from the equations, f_r being computed as 54 Hz. These theoretical lines can be compared with the experimental straight lines in Fig. 5 of DeFelice et al. (1981), for which f_r was measured as 62.2 Hz. Their lines are redrawn in Fig. 1 as broken lines. The coordinate axes of Figs. 5–10 of DeFelice et al. (1981) are not directly comparable with those in the present paper. They measured sinusoidal potentials and currents as peak-to-peak, while in this paper they are zero-to-peak. The numbers labeling both axes in their figure were therefore halved when their lines were replotted. Though the agreement is not accurate, the theoretical lines lie fairly close to the experimental ones, to within half an order of magnitude.

In Fig. 2, the six frequency values at the upper right label the theoretical (solid) lines that end there. For the slope 1 lines (above), the minimum current occurs at f_r (54 Hz), and lines at two other frequencies (one higher and one lower) give somewhat higher currents. The slope 2 lines (below) occur in a different order with respect to frequency, with the one for f_r in the middle. These theoretical lines lie fairly close to the experimental lines in Fig. 7 of DeFelice et al. (1981), for which $f_r = 67.7$ Hz, replotted here as broken lines. (Notice that the slope 2 lines in their figure are labeled with twice the fundamental frequency $2f$, but here with the fundamental frequency f.)

Fig. 3 *a* shows $|I_2|$, the theoretical amplitude of the second-order admittance defined in Eq. 22, plotted against

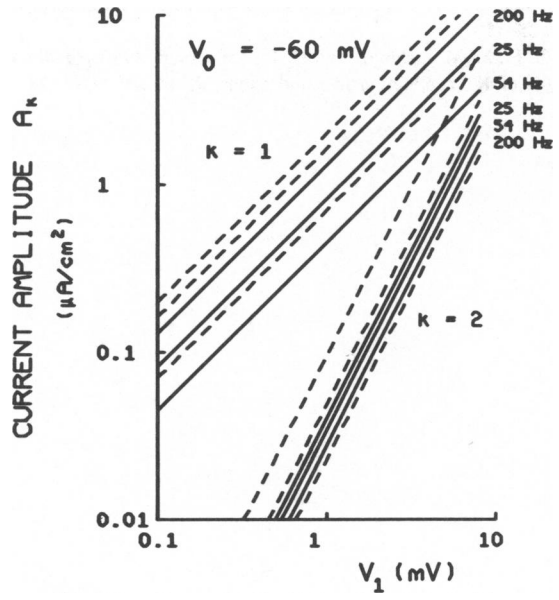

FIGURE 2 Theoretical and experimental straight lines of slope 1 and 2, as in Fig. 1, but drawn for three frequencies: f_r, 25 Hz, and 200 Hz. f_r = 54 Hz (theoretical), 67.7 Hz (experimental).

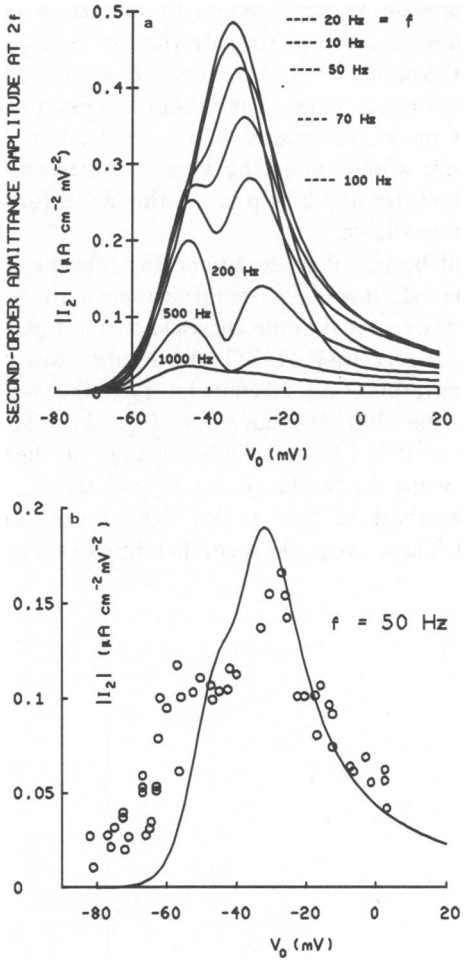

FIGURE 3 (*a*) The amplitude $|I_2|$ of the second-order admittance at $2f$, for eight different frequencies f, plotted against the DC amplitude V_0 of the voltage-clamp step. (*b*) Experimental data from L. J. DeFelice and W. J. Adelman (unpublished), plotted as circles, for f = 50 Hz. The theoretical curve is scaled for comparison. See text. Theoretical resting potential −60 mV.

V_0, the voltage step amplitude, for different frequencies f. Some of these curves have two humps, which appear most distinctly for intermediate values of frequency.

The curve for frequency $f = 50$ Hz, the only frequency for which good experimental data are available, shows merely a suggestion of a hump on its left slope. Fig. 3 *b* shows data supplied by L. J. DeFelice and W. J. Adelman (personal communication), plotted as circles. These data are from five axons in artificial sea water at 5–7°C, having resting potentials from -57 to -61 mV. The frequency f was 50–53 Hz. Further details on the experimental methods are given in DeFelice et al. (1981). The points in this figure were recomputed from their data, which were peak-to-peak values of current density measured with, in their notation, $V_p = 2.1$ to 2.15 mV (i.e., $V_1 = 1.05$ to 1.075 mV), to give values of second-order admittance, for comparison with theory.

The curve in Fig. 3 *b* is the same as the one in Fig. 3 *a* for 50 Hz, but has been rescaled vertically by multiplying by 0.45, to provide an approximate fit to their data. Their points follow a curve of roughly the same shape as the theoretical one, but their current values are less than half of the theoretical ones. Their points seem to show a somewhat more pronounced hump on the left, and are spread more widely along the V_0 axis. Measurements at other frequencies would help to test the model further, but are not yet available.

It would be useful to determine the relative contributions of the sodium and potassium currents to the nonlinear currents, as expressed in the curves shown in Fig. 3 and in Figs. 2–5 of FitzHugh (1981). An attempt was made to analyze the terms of Eq. 20 contributing to the two distinct peaks of the 200 Hz curve in Fig. 3 *a*. The term $(1/2)J_{mm}(m_1^{c1})^2$ in I_2^{c1c1} contributes strongly to the peak at -45 mV, while the two terms $J_{mm}\, m_1^{c1}\, m_1^{s1}$ and $J_{mh}\, MH_{11}^{c1s1}$ in I_2^{c1s1} contribute to both peaks. Other terms were less important. These two peaks seem therefore to result mainly from nonlinearities in the sodium current. By setting $\bar{g}_K$ or $\bar{g}_{Na}$ equal to zero in Eq. 13 and recomputing the curves one could hope to determine in more detail the separate contribution of the sodium or potassium current.

Because of the variability of the condition of experimental axons and the difference of species of *Loligo*, close quantitative agreement of the experimental measurements of frequency f_r and of membrane currents with the HH model cannot be expected. One can conclude, therefore, that the theoretical equations derived from the HH model provide a satisfactory agreement with the experimental results.

In conclusion, the higher-order sinusoidal components of the membrane current, obtained in response to a sinusoidal voltage clamp, yield generalized admittances which provide a new way to study the nonlinear properties of a nerve membrane. Unfortunately, the complexity of the mathematical expressions seems to preclude any easy intuitive interpretation of the shapes of some of the resulting curves.

Received for publication 16 September 1982 and in final form 15 November 1982.

REFERENCES

DeFelice, L. J., W. J. Adelman, D. E. Clapham, and A. Mauro. 1980. Second order admittance in squid axon. *Fed. Proc.* 39:2072.

DeFelice, L. J., W. J. Adelman, D. E. Clapham, and A. Mauro. 1981. Second order admittance in squid axon. *In* The Biophysical Approach to Excitable Systems. W. J. Adelman and D. E. Goldman, editors. Plenum Publishing Corp., New York. 37–63.

Fishman, H. M., D. Poussart, and L. E. Moore. 1979. Complex admittance of Na^+ conduction in squid axon. *J. Membr. Biol.* 50:43–63.

FitzHugh, R. 1981. Nonlinear sinusoidal currents in the Hodgkin-Huxley model. *In* The Biophysical Approach to Excitable Systems. W. J. Adelman and D. E. Goldman, editors. Plenum Publishing Corp., New York. 25–35.

Moore, L. E., H. M. Fishman, and D. J. M. Poussart. 1980. Small-signal analysis of K^+ conduction in squid axons. *J. Membr. Biol.* 54:157–164.